

Original Article

A preliminary report of gastroenteropancreatic neuroendocrine tumors in one institution: CT, MRI and clinicopathological features

Tao Lu¹, Hong Pu¹, Gao-Ping Zhao², Guang-Wen Chen¹

Departments of ¹Radiology, ²Gastrointestinal Surgery, Sichuan Academy of Medical Sciences & Sichuan Provincial People's Hospital, Chengdu 610072, Sichuan Province, China

Received June 16, 2016; Accepted August 22, 2016; Epub November 15, 2016; Published November 30, 2016

Abstract: Objective: To present the imaging and clinicopathological features of gastroenteropancreatic neuroendocrine tumors (GEP-NETs). Material and methods: Between January 2013 and December 2015, 48 patients with surgically diagnosed GEP-NETs (34 male and 14 female) underwent preoperative multidetector computed tomography or magnetic resonance imaging. The clinical and imaging features of the patients were reviewed and analyzed. Results: Pancreatic tumors are mainly located in the head and body of the pancreas. Gastrointestinal involvement included the following: 12 tumors located in the stomach, 11 in the rectum, 3 in the esophagus or colon, and 2 in the duodenum or appendix. Patients were mainly diagnosed in their 50 s to 70 s with a mean age of 61 years. The dominant clinical symptoms included abdominal pain, dysphagia, hematemesis or hematochezia and neuroendocrine-related symptoms. 20 tumors were classified as G3, 12 as G2 tumors, 11 as G1 and 5 as mixed adeno-neuroendocrine carcinoma. The immunohistochemical markers chromogranin and synaptophysin were positive. The pancreatic tumor showed iso-to hypoattenuation on plain computed tomography (CT), iso-to hypointensity on T1-weighted imaging and iso-to hyperintensity on T2-weighted imaging. The enhancement pattern was variable. The CT features of GEP-NETs mainly included wall thickening, and nodules or masses on the wall of the gastrointestinal tract. The two main enhancement patterns were moderately homogeneous and irregularly heterogeneous. 14 cases of lymph node metastases, 9 of liver, 3 of lung and one of lumbar vertebrae were also detected by CT. Conclusions: in China, the most common sites for GEP-NETs are the pancreas, stomach and rectum. The imaging features of pancreatic NETs and GEP-NETs are nonspecific.

Keywords: Gastroenteropancreatic neuroendocrine tumors, computed tomography, magnetic resonance imaging

Introduction

Gastroenteropancreatic neuroendocrine tumors (GEP-NETs) are a heterogeneous group of neoplasms that arise from cells of the diffuse neuroendocrine system. They are characterized by an indolent rate of growth and a propensity to secrete a variety of peptide hormones and biogenic amines [1]. All NETs are potentially malignant but differ in their biological characteristics and probability of metastatic disease. Although previously regarded as rare, GEP-NETs represent the second most common digestive cancer in western countries following colorectal carcinoma [2, 3]. A substantial increase in their incidence has been reported in the past four decades, which may be due to

improvements in imaging techniques and the extensive use of endoscopy [4, 5]. According to the report of the Surveillance, Epidemiology and End Result (SEER) Program of the National Cancer Institute, the annual incidence of GEP-NETs is 3.65/100000 individuals [2]. The age-adjusted incidence of GEP-NETs has also increased steadily over the last four decades, with a 3.6-fold increase occurring between 1973 and 2007 [3].

Current studies of GEP-NETs are mostly from the US and Europe, but there are limited data from Asian countries. The number of reports of GEP-NETs is gradually increasing in China. However, the registration system for neoplasms throughout the country has not been complet-

CT, MRI and clinicopathological features of GEP-NETs

Table 1. Clinical data in 48 patients with GEP-NETs, *n* (%)

Age	Location							Total
	Pancreas	Esophagus	Stomach	Duodenum	Colon	Appendix	Rectum	
< 50	3 (6.3)		1 (2.1)	1 (2.1)	1 (2.1)		3 (6.3)	9 (18.8)
50-60	4 (8.4)	2 (4.2)	3 (6.3)	1 (2.1)		1 (2.1)	3 (6.3)	14 (29.2)
60-70	5 (10.4)		7 (14.6)		2 (4.2)		4 (8.4)	18 (37.5)
> 70	3 (6.3)	1 (2.1)	1 (2.1)			1 (2.1)	1 (2.1)	14 (14.5)
Total	15 (31.3)	3 (6.3)	12 (25.0)	2 (4.2)	3 (6.1)	2 (4.2)	11 (22.9)	48 (100.0)

Table 2. Symptoms of 48 patients with GEP-NETs, *n*

Symptoms	Location							Total
	Pan-creas	Esoph-agus	Stom-ach	Duode-num	Colon	Ap-pendix	Rec-tum	
Neuroendocrine-related symptoms	8							8
Dysphagia		3	6					9
Abdominal pain	3		7	1	2	2	1	16
Abdominal distention			2		2		1	5
Hematemesis or hematochezia			3				5	8
Change of stool character and altered bowel habit							5	5

ed, thus, detailed information, including epidemiology, presentation and pattern of care of GEP-NETs, is still unclear in China. Tumor detection, characterization and staging are essential in the management of GEP-NETs and for treatment planning. Morphological imaging, such as multidetector computed tomography (MDCT) and magnetic resonance imaging (MRI) are important methods for evaluating the disease. However, there is a paucity of research on the imaging features of GEP-NETs, so the purpose of this study was to show the imaging and clinicopathological features of this disease. This study could serve as a catalyst in our effort to increase awareness of GEP-NETs and remind radiologists to consider them as an important differential diagnosis of GEP tumors.

Materials and methods

Patient characteristics

Institutional review board approval was obtained and informed consent was waived for this retrospective study. We retrospectively analyzed our database of all patients who underwent CT scanning at our hospital from January 2013 to December 2015. Forty-eight cases (34 male and 14 female) out of 141 surgically resected GEP-NETs patients were definitively diagnosed postoperatively by pathologi-

cal examination and immunohistochemistry. The patients ranged in age between 25 and 78 years, with a mean age of 61 years. Duration of symptoms prior to diagnosis ranged from 2 days to 15 years.

CT techniques

All CT examinations were performed using a SOMATOM Sensation 16 and SOMATOM Perspective Scanner (Siemens Medical Systems, Erlangen, Germany). The thickness of the scanning slices and reconstructed images were 8 and 2 mm, respectively. Non-ionic contrast material (1.5 mL/kg) with an iodine concentration of 300 mg/mL (Visipaque; GE Healthcare, Ireland) was injected at a rate of 2.5-3 mL/s through the median cubital vein. Contrast-enhanced images were obtained using a 75-s delay.

For the Sensation 16 Scanner, the imaging parameters were as follows: beam collimation of 16 × 1.5 mm, beam pitch of 1.2, gantry rotation time of 1 s, 120 kV and 180 mAs. The parameters for the Perspective Scanner were as follows: beam collimation of 64 × 0.6 mm, beam pitch of 0.8-1.2, gantry rotation time of 0.5 s, 130 kV and automated dose modulation using a maximum allowable tube current set at 200 mAs.

CT, MRI and clinicopathological features of GEP-NETs

Table 3. Pathological findings of 48 patients with GEP-NETs, *n* (%)

Location	G1	G2	G3	MANEC	Syn (+)	CgA (+)
Pancreas	5 (10.4)	5 (10.4)	5 (10.4)		15 (31.3)	13 (27.1)
Esophagus			3 (6.3)		3 (6.3)	
Stomach		2 (4.2)	8 (16.7)	2 (4.2)	11 (22.9)	12 (25.0)
Duodenum	1 (2.1)			1 (2.1)	2 (4.2)	2 (4.2)
Colon			3 (6.3)		3 (6.3)	3 (6.3)
Appendix		1 (2.1)		1 (2.1)	2 (4.2)	2 (4.2)
Rectum	6 (12.5)	3 (6.3)	1 (2.1)	1 (2.1)	10	4 (8.4)
Total	12 (25)	11 (22.9)	20 (41.7)	5 (10.4)	46 (95.8)	36 (75)

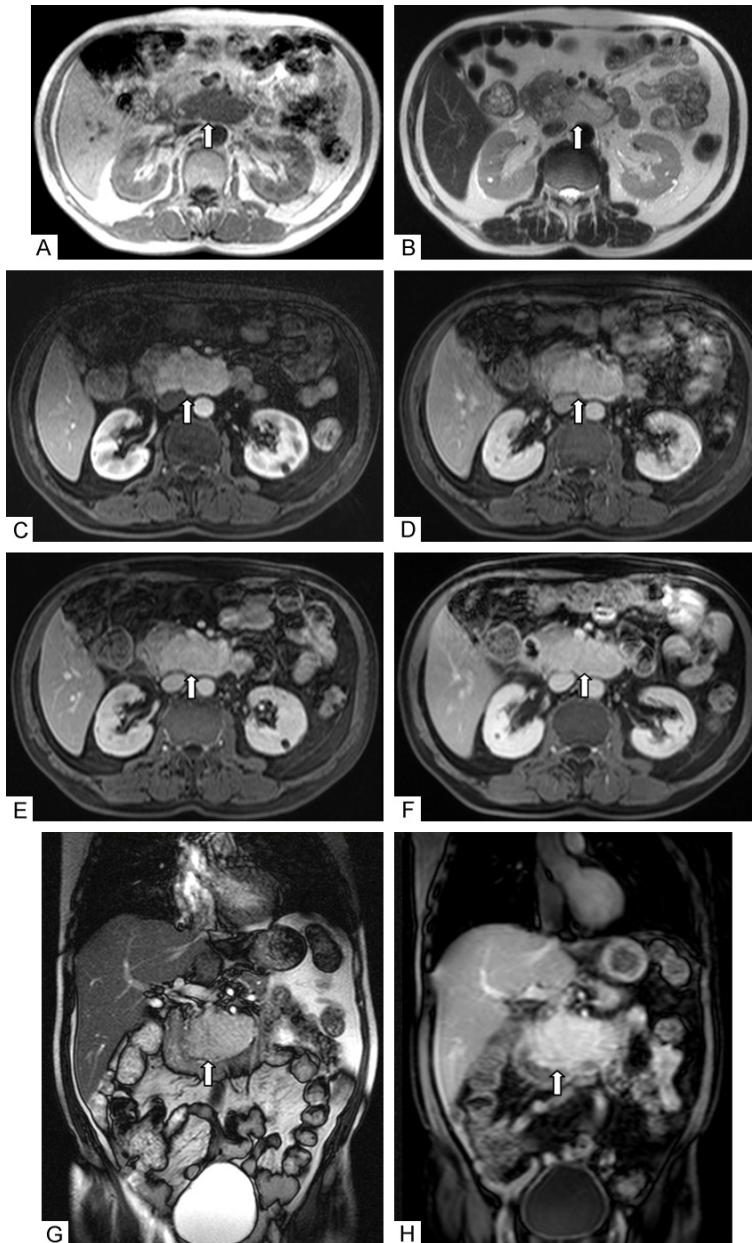


Figure 1. A-H: show MR images of a 74-year-old man with G2 pancreatic NET. T1WI (A), T2WI (B), contrast-enhanced (C-F), coronal (G, H) images showed a mass (arrow) with persistent enhancement located in the uncinus process of the head of the pancreas.

MRI techniques

MRI was performed using a 1.5-T MR system (Avanto 1.5T; Erlangen) with body array coils. Basic MRI consisted of the following sequences: (1) axial TSE-T1W (Turbo spin echo-T1 weighted image) pre-contrast (field of view 350 mm, 6-mm thick section, matrix 256 × 208, TR Repetition time, 111 ms and TE Echo time 2.38 ms); (2) TSE-T2W (Turbo spin echo-T2 weighted image field of view 350 mm, 6-mm thick section, matrix 256 × 186, TR 1000 ms and TE 85 ms); and (3) dynamic contrast-enhanced (DCE)-MRI was acquired using a prototypical VIBE (volumetric interpolated breath-hold examination) sequence (2.5-mm thick section, matrix 320 × 195, TR 4.87 ms and TE 2.83 ms). Body-weight-adapted intravenous contrast agent (Omniscan; GE Healthcare) was administered. DCE-MRI was acquired at 15, 30, 45 and 60 s after injection of the contrast agent.

Results

Clinical findings

Table 1 summarizes the age and location of the GEP-NETs in the 48 patients. Pancreas (31.25%) was the most common tumor site, followed by stomach (25%) and rectum

CT, MRI and clinicopathological features of GEP-NETs

Table 4. Imaging features of 15 patients with pancreatic NETs according to different pathological grading, *n* (%)

Grading	Location				size		Mean maximum size (cm)	Cystic or necrotic change	Shape		Enhancement pattern			Metastasis	Invasion
	Head	Neck	Body	Tail	< 2 cm	> 2 cm			Oval	Irregular	I	II	III		
G1	3 (17.6)	1 (5.7)	1 (5.7)		3 (17.6)	2 (11.8)	2.74	2 (11.8)	3 (17.6)	2 (11.8)	1 (5.7)	3 (17.6)	1 (5.7)	Liver	No
G2	1 (5.7)		3 (17.6)	1 (5.7)	3 (17.6)	2 (11.8)	4.08	4 (23.5)	3 (17.6)	2 (11.8)		4 (23.5)	1 (5.7)	Liver	No
G3	3 (17.6)		3 (17.6)	1 (5.7)	4 (23.5)	3 (17.6)	4.76	3 (17.6)	4 (23.5)	3 (17.6)		1 (5.7)	6 (35.3)	Liver, lumbar vertebra, lymph node	1 case
Total	7 (41.2)	1 (5.2)	7 (41.2)	2 (11.8)	10 (58.8)	7 (41.2)			10 (58.8)	7 (41.2)	1 (5.82)	8 (47.1)	8 (47.1)		

Note: Enhancement pattern: I (obvious enhancement during arterial phase and washout in portal venous phase); II (obvious enhancement in both arterial and portal venous phases); III (mild to moderate enhancement during arterial phase and further enhancement in portal venous phase).



Figure 2. (A-C) show CT images of a 41-year-old man with G2 rectal NET. Axial (A), coronal (B) and sagittal (C) images showed a nodule (arrow) with homogeneous enhancement on the right side of the wall of the rectum.



symptoms of the GEP-NETs in the 48 patients. Abdominal pain was the most common symptom in 18 patients, followed by dysphagia in 12, hematemesis or hematochezia in 8, and neuroendocrine-related symptoms in 8. Other symptoms included abdominal distention, change in stool character and altered bowel habit. Neuroendocrine-related symptoms including hypoglycemia, paroxysmal loss of consciousness, malaise, profuse perspiration, and repeated diarrhea were exclusively seen in pancreatic NETs. Two patients with pancreatic NETs were symptom free and tumor was detected incidentally during routine health check-up.

Pathological findings

Pathological tumor grades were determined according to the revised 2010 WHO classification. Twelve patients (25%)

(22.92%). Esophagus (6.25%), colon (6.25%), duodenum (4.17%) and appendix (4.17%) were less common sites. The detailed locations of the pancreas were: seven tumors each in the head and body, two in the tail and one in the neck of the pancreas. The detailed locations in the stomach were: six tumors in the body (4 in the lesser curvature and two in the greater curvature), three in the cardia and two in the antrum. The detailed locations in the rectum were nine tumors in the middle segment and two in the inferior segment. The detailed locations in the esophagus were two tumors in the middle segment and one in the superior segment. There was one tumor each located in the ascending, descending and sigmoid colon. Two cases of duodenal NETs were located in the papilla of Vater of the descending segment. One case of appendiceal NET was confined to the appendix itself and another invaded the ileocecal region.

The age of onset was mainly in the 60 s and 70 s (37.50%), followed by the 50 s and 60 s (29.17%). There were few patients aged < 50 and > 70 years. **Table 2** summarizes the main

were classified as G1, 11 (22.93%) as G2, 20 (41.57%) as G3, and 5 (10.42%) as mixed adenoneuroendocrine carcinoma (MANEC). Histopathological staining revealed that 95.83% of all cases were positive for synaptophysin and 75% were positive for chromogranin A. **Table 3** lists the pathological classification of GEP-NETs in different locations in detail.

Imaging findings

Among 15 patients with pancreatic NETs, one had three tumors and the other 14 had a single tumor each. In all, 17 tumors were detected. Tumor lesions were located in the head ($n = 7$), neck ($n = 1$), body ($n = 7$) and tail ($n = 2$) of the pancreas. Tumor size was < 20 mm in nine lesions and > 20 mm in eight. The maximum tumor diameter was 1-16 cm, and median maximum tumor diameter was 3.12 cm. The maximum tumor diameter of six lesions was > 5 cm. Calcification was observed only in one tumor. Cystic or necrotic change was observed in nine lesions. The tumor shape was oval in nine lesions and irregular in eight. Nine tumors were within the pancreas and eight exceeded the

CT, MRI and clinicopathological features of GEP-NETs

Table 5. Enhancement pattern of 33 patients with GEP-NETs, *n* (%)

Location	Case no	Enhancement pattern				
		Heterogeneous enhanced		Homogeneous enhanced		
		Peripherally enhanced	Irregularly enhanced	Slightly enhanced	Moderately enhanced	Obvious enhanced
Esophagus	3		1 (3.0)	1 (3.0)	1 (3.0)	
Stomach	12		4 (12.1)	2 (6.1)	4 (12.1)	2 (6.1)
Duodenum	2		1 (3.0)		1 (3.0)	
Colon	3		3 (9.1)			
Appendix	2			2 (6.1)		
Rectum	11	2 (6.1)	2 (6.1)	1 (3.0)	6 (18.2)	
Total	33	2 (6.1)	11 (33.3)	6 (18.2)	12 (36.4)	2 (6.1)

extent of the pancreas. The tumor was iso- or hypoattenuated on plain CT scanning. Six lesions showed hypointensity on T1-weighted imaging (T1WI) and hyperintensity on T2-weighted imaging (T2WI); two lesions showed hypointensity on T1WI and isointensity on T2WI; and one lesion showed isointensity on both T1WI and T2WI. One case of pancreatic NET demonstrated obvious enhancement during the arterial phase and washout in the portal venous phase. Eight cases demonstrated obvious enhancement in both the arterial and portal venous phases. Six cases (8 lesions) demonstrated mild to moderate enhancement during the arterial phase and further enhancement in the portal venous phase (**Figure 1A-H**). One case of G3 pancreatic NET invaded the spleen, splenic hilum, left kidney and left perirenal space. Liver metastasis was observed in one case each of G1 and G2 tumor. One case of liver metastasis accompanied by lumbar vertebral metastasis was observed in one case of G3 tumor. One case of lymphadenopathy in the portal caval space was detected in a G3 tumor (**Table 4**).

The wall was circumferentially thickened and the lumen was slightly narrowed in esophageal NETs. Enlargement of the esophageal lymph nodes and liver metastases were also detected in one case. The wall was thickened in seven cases of gastric NETs (evenly thickened in 6 and unevenly thickened in 1). Four cases were manifested as gastric masses or nodules (> 2 cm, 2 cases were exophytic, 1 formed a mass inside the lumen, and 1 formed a nodule in the wall accompanied by thickening of the wall). Two cases of duodenal NETs consisted of nodules in the lumen of the descending duodenum.

The wall was slightly thickened and the surrounding fat interspace was obscure in one case of appendiceal NETs. In a case of appendiceal NET, the wall was thickened in the area of the ileocecal junction. Two cases of colonic NETs were manifested as uneven thickening of the wall and formation of a mass with invasion to adjacent structures. The other case of colonic NET had similar uneven thickening of the wall with the surrounding fat interspace blurred. In 11 cases of rectal NET, three showed thickening of the wall (uneven in 2 cases and circular in 1); four had wall thickening and nodular protrusion (**Figure 2A-C**); and one each had nodular protrusion and exophytic nodules. Three cases each had nodule size < 2 cm and > 2 cm. The enhancement pattern of 33 cases of GEP-NETs is listed in **Table 5**. Twelve cases (36.36%) appeared as moderately homogeneous enhancement and 11 (33.33%) as irregular enhancement. CT detected 13 cases of lymphadenopathy (6 regional metastatic lymphadenopathy, 1 distant metastatic lymphadenopathy, and 6 both regional and distant lymphadenopathy), six cases of liver metastases, and three of lung metastases.

Discussion

GEP-NETs are a heterogeneous and complex group of neoplasms with a wide spectrum of clinical manifestations. The tumor distribution in the body varies in different parts of the world. In the US, GEP-NETs are most common in the small intestine, followed by the rectum, colon, pancreas and appendix [5]. However, according to several large retrospective studies from China, GEP-NETs are most common in the pancreas, followed by the rectum and appendix,

CT, MRI and clinicopathological features of GEP-NETs

and the small intestine is an uncommon location [6]. Epidemiological studies from the US and Japan indicated that the distribution of GEP-NETs differed between Asian and Caucasian populations, but it was unclear whether this was related to racial differences. In the US, pancreatic NETs only account for 7% of all GEP-NETs. Guo and Tang [7] summarized all the relevant references from 1954 to 2011 in China and found that pancreatic NETs were the most common form of the disease, accounting for 49.8% of all cases. In the present study, the pancreas (31.25%) was also the most common site of the disease, followed by the stomach (25%) and rectum (22.92%), and the esophagus, duodenum, appendix and colon were less common sites.

In 1907, the German pathologist Oberndorfer first introduced the nomenclature "carcinoid" or "carcinoid tumor". Historically, there were several classifications to categorize NETs. However, this led to confusion and miscommunication between physicians, radiologists and pathologists. In response, attempts have been made to organize and categorize the tumors that comprise the neuroendocrine disease spectrum. In 2000, the WHO published a classification for GEP-NETs and modified it in 2010 to include tumor grade and differentiation. The term carcinoid was rejected and replaced by NET in the updated classification. GEP-NETs were divided into five categories: (1) NET G1 (low-grade malignancy); (2) NET G2 (intermediate-grade malignancy); (3) neuroendocrine carcinoma G3 (high-grade malignancy); (4) MANEC; and (5) hyperplastic and preneoplastic lesions. In this study, G3 tumors (41.67%) were the most frequent, followed by G1 (25%), G2 (22.92%) and MANEC (10.42%). Three-quarters of gastric tumors were G3; esophageal and colonic NETs were all G3; and more than half the rectal NETs were G1 with only one case of G3. Immunohistochemical staining has played an important role in diagnosis of NETs. General neuroendocrine markers chromogranin A and synaptophysin are widely used and recommended by current guidelines. Elevated chromogranin A and synaptophysin can be detected in 70-90% of GEP-NETs, and it is reported that positivity for chromogranin A and synaptophysin was 70.6% and 94.1%, respectively [8]. In the present study, positivity for chromogranin A and synaptophysin was 75% and 95.83%,

respectively, which is similar to previous reports.

The incidence of GEP-NETs has increased markedly in recent years with the increase in the aging population. Data from the US indicate that there is a higher overall incidence in men (52%) compared with women (48%), with the median age at diagnosis of 63 years [2, 3, 9]. According to data from China, the incidence ratio of male: female was 1.2: 1 and the median age was 50 years [7]. In this study of 48 cases of GEP-NETs, the incidence ratio of male: female was 2.43: 1 and the median age was 61 years. Patients in their 50s and 60s (68.67%) were principally affected. Relatively fewer patients younger than their 50s or older than their 70s were affected. It seems that GEP-NETs have a tendency to occur in elderly men.

GEP-NETs present as hormonally functioning or non-functioning tumors. Most tumors are non-functioning in China and the classic carcinoid syndrome only develops in rare cases. Most pancreatic NETs are functioning. Insulinomas and gastrinomas are the most common types; they can secrete insulin or gastrin, respectively, and cause distinct clinical syndromes. However, the majority of GEP-NETs are non-functioning and lack secretion of peptide hormones. Most of the cases do not have neuroendocrine-related symptoms and are often diagnosed when symptoms of mass effects or even metastases develop. The most common symptoms in our patients were abdominal pain, dysphagia, hematemesis and hematochezia, and neuroendocrine-related symptoms. Eight cases with neuroendocrine-related symptoms were exclusively functioning pancreatic NETs. Other less common symptoms included abdominal distention, change of stool character, and altered bowel habit. In the seven cases of non-functioning pancreatic NETs, five mainly complained of abdominal pain, and the other two were symptom free and were detected incidentally during routine health check-up. In esophageal and gastric NETs, the main symptoms were abdominal pain and dysphagia, while in rectal NETs, the main symptoms were hematemesis or hematochezia, abdominal distention, change of stool character, and altered bowel habit.

Pancreatic NETs are usually located in the head, body and tail of the pancreas, and are round or oval. Calcification, cystic or necrotic

CT, MRI and clinicopathological features of GEP-NETs

changes can present, making the tumor heterogeneous. The lesions can be small and limited to the pancreas, but they can also be large in size, leading to contour deformity. Typical pancreatic NETs are hypervascular and show intense enhancement during the arterial phase. The above morphology on CT images can also be seen on MR images. In addition, pancreatic NETs appear as iso-to hypointense masses on T1WI and iso-to hyperintense on T2WI. In our study, pancreatic NETs were usually located in the head and body of the pancreas. Calcification was observed only in one tumor, and cystic or necrotic change was observed in nine. There were several enhancement patterns in the tumors. The most common enhancement patterns were obvious enhancement during both the arterial and portal venous phases, and mild to moderate enhancement during the arterial phase and further enhancement during the portal venous phase. G2 and G3 pancreatic NETs were larger than G1 tumors. G1 tumors were inclined to be present within the pancreas and G3 tumors usually exceeded the extent of the pancreas. The enhancement pattern of G1 and G2 tumors was mainly obvious enhancement during both the arterial and portal venous phases, while G3 tumors had mild to moderate enhancement during the arterial phase and further enhancement during the portal venous phase.

The CT features of GEP-NETs are non-specific. Local thickening of the wall, nodular protrusion and soft tissue mass are common features of lesions > 1 cm. Necrosis can be found in large masses. The dominant CT feature of gastric NETs was even thickening of the wall. Thickening of the wall and nodule formation in the wall were both common in rectal NETs. Diffuse circumferential wall thickening was seen in esophageal NETs and intraluminal nodules were observed in duodenal NETs. Colonic NETs usually manifested as uneven thickening of the wall and formation of mass-like tumors. NETs in the appendix also manifested with thickening of the wall, and the ileocecal junction may also have been involved. NETs typically have a rich blood supply. However, obvious enhancement was less common in GEP-NETs than in pancreatic NETs. Instead, GEP-NETs always demonstrated moderately homogeneous enhancement. When the lesion grew large, necrosis was

common, and irregular heterogeneous enhancement was dominant in such lesions.

All GEP-NETs are potentially malignant, but the probability of metastasis is different. Even low-grade malignant tumors can metastasize and invade adjacent structures. The judgment of biological characteristics of NETs with imaging mostly relies on detection of metastases to the liver and lymph nodes or invasion to the adjacent structures. Regional and distant disease spread is reported in 20-40% of cases [2]. Non-functioning tumors of the pancreas and gastrointestinal tract are more likely to metastasize [10, 11]. The most common metastatic sites are the lymph nodes and liver, followed by lung, bone, peritoneum and mesentery, soft tissue, brain and breast [12]. In the present study, regional and distant disease spread was detected in 16 of 48 cases, including regional and distant metastatic lymphadenopathy, and liver, lung and lumbar vertebral metastases. The secondary lesions, most notably liver metastases, tend to show a similar imaging pattern as the primary lesion. The hepatic lesions are usually hypervascular in the arterial phase, with circular enhancement and washout in the late phase [11, 13]. Less frequently, they show transient homogeneous enhancement in the arterial phase or mild enhancement in the portal venous and delayed phases. In the present study, only one case of liver metastasis showed homogeneous enhancement in the arterial phase and washout in the venous phase.

Complete surgical resection is the first line and potentially curative treatment of primary GEP-NETs regardless of their origin. The surgical approach is influenced by lesion size and location, disease stage and the patient's symptoms. Limited resection under endoscopy is considered when the lesion is < 2 cm and non-invasive. Radical surgery along with resection of draining lymph nodes is recommended for lesions > 2 cm or invasive, or when the muscularis mucosa is involved. Partial hepatic resection can be performed concurrently with primary tumor removal. Imaging strongly contributes to patient care and its role mostly involves detection and characterization of the primary lesions, staging and subsequent follow-up [14]. Morphological imaging, MDCT and MRI are also the most widely used techniques for initial evaluation and detection of metastatic disease.

CT, MRI and clinicopathological features of GEP-NETs

Reports of GEP-NETs have increased in recent years. Clinicians are paying more attention to this not-so-rare disease now. However, research on its imaging features is rare. The present study had several limitations. First, our study was retrospective and the observers were aware of the diagnosis. Second, this study included a small number of patients. The numbers of G1 and G2 tumors were small, which may have been because most G1 and G2 tumors presented only as small polyps and were resected under endoscopy, so the patients did not undergo further CT.

In conclusion, GEP-NETs mainly involve elderly men in their 50 s and 60 s. The pancreas, stomach and rectum are the most common sites of the disease in China. The dominant symptoms include abdominal pain, dysphagia, hematemesis or hematochezia, and neuroendocrine-related symptoms. Pancreatic NETs showed iso-to hypoattenuation on plain CT scanning, iso-to hypointensity on T1WI, and iso-to hyperintensity on T2WI. The two main enhancement patterns included obvious enhancement in both the arterial and portal venous phases, and mild to moderate enhancement during the arterial phase and further enhancement during the portal venous phase. The common CT features of GEP-NETs include wall thickening, and nodule or mass formation on the wall of the gastrointestinal tract. The two main enhancement patterns are moderately homogeneous and irregular heterogeneous enhancement. CT can also sensitively detect lymph node, liver and lung metastases of the GEP-NETs.

Disclosure of conflict of interest

None.

Authors' contribution

Lu T, Pu H, Zhao GP, Chen GW contributed equally to this work: (1) Conception and design: Zhao GP; (2) Administrative support: Pu H; (3) Provision of study materials or patients: Lu T; (4) Collection and assembly of data: Lu T; (5) Data analysis and interpretation: Chen GW; (6) Manuscript writing: All authors. (7) Final approval of manuscript: All authors.

Address correspondence to: Dr. Gao-Ping Zhao, Department of Gastrointestinal Surgery, Sichuan Academy of Medical Sciences & Sichuan Provincial

People's Hospital, 32 West Second Section, First Ring Road, Chengdu 610072, Sichuan Province, China. Tel: +86-18981838575; Fax: +86-028-87394279; E-mail: gzhao@uestc.edu.cn; Dr. Hong Pu, Department of Radiology, Sichuan Academy of Medical Sciences & Sichuan Provincial People's Hospital, Chengdu 610072, Sichuan Province, China. Tel: 86-18981838657; Fax: 86-28-8739-4279; E-mail: ph1726148853@qq.com

References

- [1] Modlin IM, Champaneria MC, Bornschein J and Kidd M. Evolution of the diffuse neuroendocrine system-clear cells and cloudy origins. *Neuroendocrinology* 2006; 84: 69-82.
- [2] Yao JC, Hassan M, Phan A, Dagohoy C, Leary C, Mares JE, Abdalla EK, Fleming JB, Vauthey JN, Rashid A and Evans DB. One hundred years after "carcinoid": epidemiology of and prognostic factors for neuroendocrine tumors in 35,825 cases in the United States. *J Clin Oncol* 2008; 26: 3063-3072.
- [3] Fraenkel M, Kim M, Faggiano A, de Herder WW and Valk GD. Incidence of gastroenteropancreatic neuroendocrine tumours: a systematic review of the literature. *Endocr Relat Cancer* 2014; 21: R153-163.
- [4] Turaga KK and Kvols LK. Recent progress in the understanding, diagnosis, and treatment of gastroenteropancreatic neuroendocrine tumors. *CA Cancer J Clin* 2011; 61: 113-132.
- [5] Lawrence B, Gustafsson BI, Chan A, Svejda B, Kidd M and Modlin IM. The epidemiology of gastroenteropancreatic neuroendocrine tumors. *Endocrinol Metab Clin North Am* 2011; 40: 1-18, vii.
- [6] Tang CW, Guo LJ. Current clinical practice of gastroenteropancreatic neuroendocrine neoplasm in China. *Zhonghua Shi Yong Waike Za Zhi* 2014; 34: 490-492.
- [7] Guo LJ, Tang CW. Current status of clinical research on gastroenteropancreatic neuroendocrine tumors in China. *Chin J Gastroenterol* 2012; 17: 276-278.
- [8] Wang CH. Clinical features of neuroendocrine tumors in digestive systems. *World Chinese Journal of Digestology* 2008, 16: 2788-2791.
- [9] Oberg K, Akerström G, Rindi G, Jelic S. ESMO guidelines working group. Neuroendocrine gastroenteropancreatic tumors: ESMO clinical practice guidelines for diagnosis, treatment and follow-up. *Ann Oncol* 2010; 21 Suppl 5: v223-227.
- [10] Wang D, Zhang GB, Yan L, Wei XE, Zhang YZ, Li WB. CT and enhanced CT in diagnosis of gastrointestinal neuroendocrine carcinomas. *Abdom imaging* 2012; 37: 738-745.

CT, MRI and clinicopathological features of GEP-NETs

- [11] Elsayes KM, Menias CO, Bowerson M, Osman OM, Alkharouby AM, Hillen TJ. Imaging of carcinoid tumors: spectrum of findings with pathologic and clinical correlation. *J Comput Assist Tomogr* 2011; 35: 72-80.
- [12] Sahani DV, Bonaffin PA, Castillo CFD, Blake MA. Gastroenteropancreatic neuroendocrine tumors: role of imaging in diagnosis and management. *Radiology* 2013; 266: 38-61.
- [13] Heller MT, Shah AB. Imaging of neuroendocrine tumors. *Radiol Clin North Am* 2011; 49: 529-548.
- [14] Dromain C, de Baere T, Lumbroso J, Caillet H, Laplanche A, Boige V, Ducreux M, Duvillard P, Elias D, Schlumberger M, Sigal R, Baudin E. Detection of liver metastases from endocrine tumors: a prospective comparison of somatostatin receptor scintigraphy, computed tomography, and magnetic resonance imaging. *J Clin Oncol* 2005; 23: 70-78.